

See discussions, stats, and author profiles for this publication at: <https://www.researchgate.net/publication/259488278>

# Enantiomeric Separations of Chiral Sulfonic and Phosphoric Acids with Barium-Doped Cyclofructan Selectors via an Ion Interaction Mechanism

ARTICLE *in* ANALYTICAL CHEMISTRY · DECEMBER 2013

Impact Factor: 5.64 · DOI: 10.1021/ac403686a · Source: PubMed

---

CITATIONS

6

---

READS

31

## 6 AUTHORS, INCLUDING:



[Jonathan P Smuts](#)

VUV Analytics, Inc.

17 PUBLICATIONS 64 CITATIONS

[SEE PROFILE](#)



[Daniel W. Armstrong](#)

University of Texas at Arlington

678 PUBLICATIONS 24,430 CITATIONS

[SEE PROFILE](#)

# Enantiomeric Separations of Chiral Sulfonic and Phosphoric Acids with Barium-Doped Cyclofructan Selectors via an Ion Interaction Mechanism

Jonathan P. Smuts,<sup>†</sup> Xin-Qi Hao,<sup>‡,§</sup> Zhaobin Han,<sup>‡</sup> Curran Parpia,<sup>†</sup> Michael J. Krische,<sup>‡</sup> and Daniel W. Armstrong\*,<sup>†</sup>

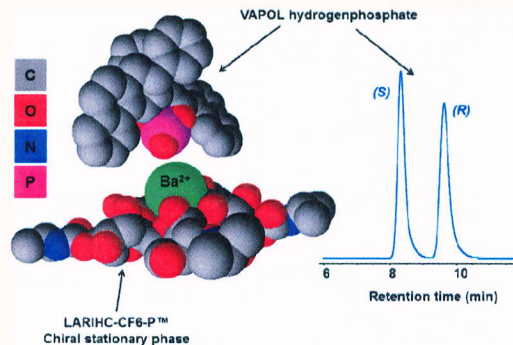
<sup>†</sup>Department of Chemistry and Biochemistry, University of Texas at Arlington, TX 76019, United States

<sup>‡</sup>Department of Chemistry and Biochemistry, University of Texas at Austin, Austin, Texas 78712, United States

<sup>§</sup>College of Chemistry and Molecular Engineering, Zhengzhou University, Zhengzhou 450052, P. R. China

## Supporting Information

**ABSTRACT:** New cyclofructan-6 (CF6)-based chiral stationary phases (CSPs) bind barium cations. As a result, the barium-complexed CSPs exhibit enantioselectivity toward 16 chiral phosphoric and sulfonic acids in the polar organic mode (e.g., methanol or ethanol mobile phase containing a barium salt additive). Retention is predominantly governed by a strong ionic interaction between the analyte and the complexed barium cation as well as hydrogen bonding with the cyclofructan macrocycle. The  $\log k$  versus  $\log [X]$ , where  $[X] =$  the concentration of the barium counteranion, plots for LARIHC-CF6-P were linear with negative slopes demonstrating typical anion exchange behavior. The nature of the barium counteranion also was investigated (acetate, methanesulfonate, trifluoroacetate, and perchlorate), and the apparent elution strength was found to be acetate > methanesulfonate > trifluoroacetate > perchlorate. A theory based upon a double layer model was proposed wherein kosmotropic anions are selectively adsorbed to the cyclofructan macrocycle and attenuate the effect of the barium cation. van't Hoff studies for two analytes were conducted on the LARIHC-CF6-P for three of the barium salts (acetate, trifluoroacetate, and perchlorate), and the thermodynamic parameters governing retention and enantioselectivity are discussed. Interestingly, for the entropically driven separations, enantiomeric selectivity can increase at higher temperatures, even with decreasing retention.



The separation of chiral phosphoric and sulfonic acid enantiomers is of great importance to synthetic and analytical chemists. The independent work of Akiyama<sup>1</sup> and Terada<sup>2</sup> in developing BINOL-phosphates to catalyze enantioselective C–C bond formation reactions in 2004 set the stage for asymmetric catalysis in a significant way.<sup>3</sup> Since then, great strides have been made in developing asymmetric catalysis for many reactions, including organocatalytic aryl–aryl bond formation,<sup>4</sup> spiroketalizations,<sup>5</sup> Mannich reactions,<sup>6</sup> hydrocyanation of hydrazones,<sup>7</sup> reductive amination,<sup>8</sup> and in crotylation reactions.<sup>9,10</sup> Chiral sulfonic acids, on the other hand, while also being strong Brønsted acids, have not enjoyed the same success in asymmetric synthesis but have rather been the focus of chiral-resolving agents in the separation of basic compounds. Recently, Kellogg et al. broadened the concept of diastereomeric recrystallization from using a single chiral selector for purifying basic racemates to simultaneously using a family of enantiomers.<sup>11</sup> This technique has been dubbed “Dutch resolution” and preferably requires three enantiomerically pure sulfonic acids from the same family (e.g., *R*-camphorsulfonic acid and *R*-bromocamphorsulfonic acid) to recrystallize basic compounds.<sup>11–13</sup> Thus, the synthesis and

separation of sulfonic acid enantiomers is important to this field.

Cyclofructan 6 (CF6) is a cyclic oligosaccharide produced by the enzymatic digestion of inulin. It consists of an 18-crown-6 core, spiro-annulated with D-fructofuranose pendant groups. Since the discovery of cyclofructans in 1989 by Kawamura et al.,<sup>14</sup> the interest in these macrocycles slowly increased. Research was primarily focused on assessing the ionophoric ability of CF6,<sup>15–18</sup> and nothing was conducted from a chromatographic perspective. In contrast to related cyclic oligosaccharides, the cyclodextrins, and even to synthetic crown ethers, cyclofructans have yet to reach the cusp of their research potential. In 2009, we published the first major chiral separations work with cyclofructans.<sup>19</sup> Subsequently, this work has been further developed and greatly expanded.<sup>20–28</sup> It was clear that native CF6 bonded to silica gel was usually a poor chiral selector. However, upon derivitization with an isopropyl carbamate group, it exhibited pronounced and broad

**Received:** November 13, 2013

**Accepted:** December 17, 2013

**Published:** December 27, 2013

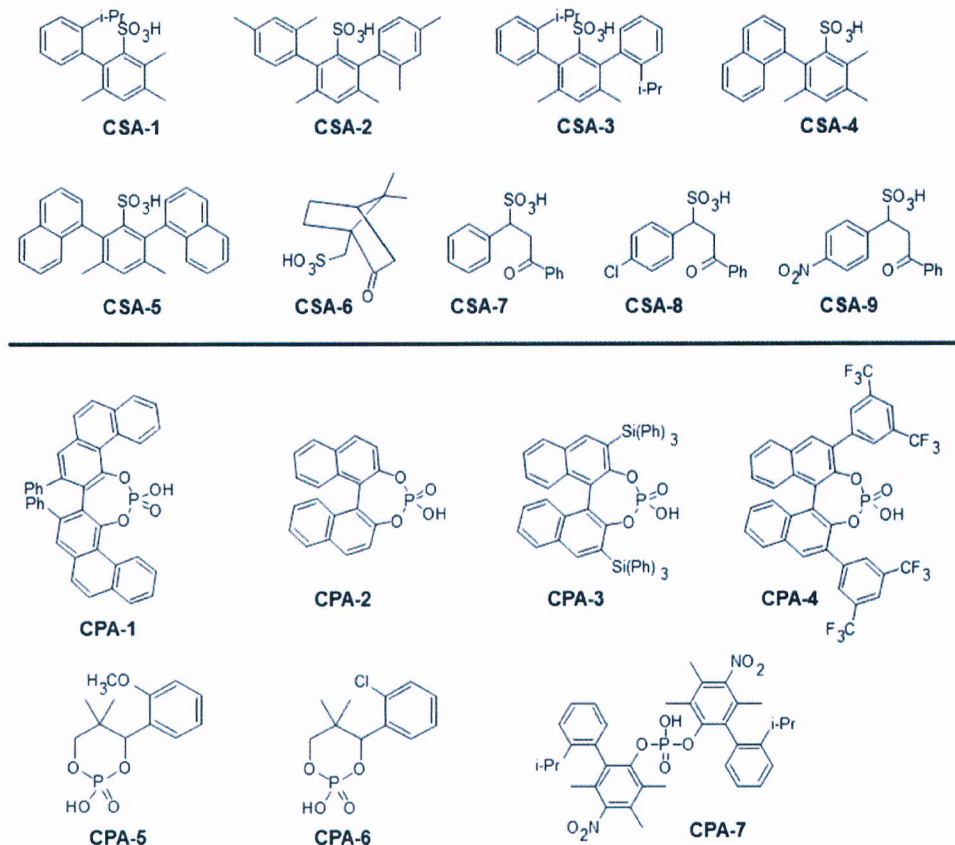


**Figure 1.** Structures of the chiral sulfonic and phosphoric acids used in this study. See text for the names of the structures.

selectivity for primary amines in organic and supercritical fluid mobile phases.<sup>19</sup> However, this selectivity did not extend to anionic or acidic compounds. It is known that the ionophoric proclivity of CF<sub>6</sub> is particularly pronounced for barium and lead cations.<sup>29</sup> Thus, the question arises as to whether this cation affinity might be exploited somehow to induce a different kind of enantioselectivity. This question is interesting from both a mechanistic point of view and from the practical standpoint that these CSPs have excellent preparative capabilities. Herein, we describe the first highly effective metal ion interaction approach for chiral separations since the classic ligand exchange work of Davankov.<sup>30,31</sup> However, the nature of the metal ion, the mechanism, and the selectivity in this work are shown to be unique. More specifically, this transforms a neutral chiral selector into one with a great affinity for anionic (sulfonic and phosphoric acid) chiral compounds. It should be noted that the analytes in this work are retained either by: (1) ion pairing with the barium cations in the mobile phase or (2) by dynamic anion exchange (i.e., where the cations, Ba<sup>2+</sup> in this case, are so strongly bound that they can be considered an integral part of the stationary phase) or (3) a combination of both ion pairing and dynamic anion exchange. Historically, the term ion-interaction chromatography has been coined to encompass but not distinguish between all of the aforementioned possibilities, particularly in reversed-phase chromatography.<sup>32</sup>

In previous work, Lindner et al. have shown using methanol mobile phases with acid/base additives that excellent separations of  $\alpha,\beta$ , and  $\gamma$ -aminophosphonic acids and chiral sulfonic acids (CSAs) can be attained on cinchona alkaloid chiral

stationary phases (CSPs).<sup>33,34</sup> Thus far we know of no other enantioselective anion-exchange-type CSPs commercially available, which makes this an important area of research.

## ■ EXPERIMENTAL SECTION

Barium acetate (Ba(OAc)<sub>2</sub>), barium hydroxide monohydrate, barium perchlorate (Ba(ClO<sub>4</sub>)<sub>2</sub>) (NOTE: all barium salts, with the exception of barium sulfate, are toxic and need to be handled with care), ammonium acetate (NH<sub>4</sub>OAc), ammonium trifluoroacetate (NH<sub>4</sub>TFA), triethylamine (TEA), trifluoroacetic acid (TFA), acetic acid (HOAc), methane sulfonic acid (MSA), ethylene diamine, (S)- and (R)-(−)-VAPOL hydrogen-phosphate (CPA-1), (S)- and (R)-(−)-1,1'-binaphthyl-2,2'-diyl hydrogenphosphate (CPA-2), (S)- and (R)-(−)-3,3'-bis(triphenylsilyl)-1,1'-binaphthyl-2,2'-diyl hydrogenphosphate (CPA-3), (S)- and (R)-3,3'-bis[3,5-bis(trifluoromethyl)phenyl]-1,1'-binaphthyl-2,2'-diyl hydrogenphosphate (CPA-4), (S)- and (R)-(+)2-hydroxy-4-(2-methoxyphenyl)-5,5-dimethyl-1,3,2-dioxaphosphorinane 2-oxide (CPA-5), (S)- and (R)-(+)4-(2-chlorophenyl)-2-hydroxy-5,5-dimethyl-1,3,2-dioxaphosphorinane 2-oxide (CPA-6), camphor sulfonic acid (CSA-6), *trans*-chalcone, 4-chlorochalcone, and 4-nitrochalcone were purchased from Sigma-Aldrich (St. Louis, MO). The total syntheses for compounds CSA-1–CSA-5 and CPA-7 together with the <sup>1</sup>H- and <sup>13</sup>C NMR, ESI-MS, and FT-IR spectra are available in the Supporting Information. Compounds CSA-7–CSA-9 were synthesized from the corresponding chalcones according to literature procedures.<sup>11,33</sup> The chiral sulfonic and phosphoric acids (see Figure 1) may be further subdivided as (1) chiral aryl sulfonic acids with either one (CSA-1 and CSA-

4) or two (CSA-2, CSA-3, and CSA-5) chiral axes, (2)  $\beta$ -ketosulfonic acids (CSA-7 – 9), and (3)  $\gamma$ -ketosulfonic acid (CSA-6). The CPAs may also be further classified as (1) biaryl phosphoric acids (CPA-1 – 4), (2) cyclic phosphoric acids (CPA-5 and 6), and (3) acyclic phosphoric acid (CPA-7). Barium trifluoroacetate ( $\text{Ba}(\text{TFA})_2$ ) was prepared by neutralizing barium hydroxide monohydrate with an excess of trifluoroacetic acid and then allowed to evaporate to dryness. The resulting residue was further dried in a vacuum oven overnight and used without further purification. When not in use, the material was stored in a desiccator. Barium methanesulfonate was prepared in an analogous way using methanesulfonic acid and barium hydroxide. HPLC grade methanol (MeOH), ethanol (EtOH), acetonitrile (ACN), and heptane (Hept) were purchased from VWR (Sugarland, TX). Water was purified by a Milli-Q-water purification system (Millipore, Billerica, MA).

**HPLC.** The HPLC used was an Agilent 1200 HPLC (Agilent Technologies, Palo Alto, CA) consisting of a diode array detector, a temperature-controlled column chamber, auto sampler, quaternary pump, and fraction collector. Data acquisition and analysis was controlled by ChemStation software (Rev. B.03.02[341], Agilent Technologies 2001–2008) in Microsoft Windows XP Professional OS. Unless stated otherwise, all HPLC separations were carried out at 25 °C with an injection volume of 5  $\mu\text{L}$  and a flow rate of 1.0 mL/min (isocratic). The following UV wavelengths were monitored: 230, 254, 265, 280, and 287 nm.

Enantiomeric separations were evaluated and optimized on barium-doped LARIHC–CF6-P (isopropyl carbamate), LARIHC–CF6-RN (*R*-1-(1-naphthyl)ethylcarbamate), and FRULIC-N (native cyclofructan) chiral CSPs 250 mm × 4.6 mm × 5  $\mu\text{m}$  (Azyp, LLC, Arlington, TX) in the polar organic mode. The polar organic mode (sometimes referred to as the polar ionic mode) mobile phase consisted of methanol (or ethanol) containing a barium salt and when necessary, varying mixtures of acidic (HOAc, TFA, or MSA) and basic (TEA, ethylene diamine) additives or ammonium salts. The void time,  $t_0$ , was measured by injecting 1,3,5-tri-*tert*-butylbenzene and monitored at 254 nm. All analytes were dissolved in methanol at ~1–2 mg/mL and stored in a freezer when not in use. CSA-6, however, was prepared in the 8–10 mg/mL range in water on account of its low UV absorbance and was monitored at 287 nm. All mobile phases were degassed by sonication under vacuum. Columns had to be conditioned by circulating the mobile phase overnight.

**Preparative HPLC.** Preparative HPLC was performed on a Jasco 2000 series HPLC using a FRULIC-N column (Azyp, LLC, Arlington, TX; 250 mm × 21 mm × 5  $\mu\text{m}$ ) treated with barium (software: Jasco ChromNav version 1.17.01). The pump (PU-2086) was set at 20 mL/min with the mobile phase consisting of methanol with 0.1% TFA and 0.1% TEA. Detection was monitored at 280 nm with a high-pressure UV-vis VWD (UV-2075) cell. The enantiomeric fractions were manually collected using the Jasco SCF-Vch-Bp 6-valve change unit. Sample injection was performed using an autosampler (AS-2059-SFC) with a 1 mL injection loop in the partial fill loop mode (injection volume = 800  $\mu\text{L}$ ).

**van't Hoff Plots.** The van't Hoff experiments were conducted at 10, 20, 30, 40, and 50 °C in a thermostatted column chamber equipped with a Peltier cooler. When the temperature was changed, the column was allowed to equilibrate for at least 30 min before injecting the samples.

The cyclofructan loading and phase ratio,  $\phi$ , where  $\phi = V_s/V_m$  ( $V_s$  = volume of the selector,  $V_m$  = volume of the mobile phase) was required for the determination of entropy from the  $\ln k$  versus  $1000/T$  plot and was calculated as published in the literature.<sup>35,36</sup> The values for the density of the LARIHC–CF6-P stationary phase and the unbonded chiral selector were measured by pycnometry (10 mL pycnometer), which was calibrated gravimetrically with DI water.

**Barium Loading and Removal.** Analytical columns were preconditioned with a 5 mM  $\text{Ba}(\text{OAc})_2$  or  $\text{Ba}(\text{TFA})_2$  solution containing 20% methanol by volume for 30 min. The preparative FRULIC-N column was preconditioned overnight with a 40 mM  $\text{Ba}(\text{OAc})_2$  solution containing 20% methanol by volume. The columns were then either evaluated directly in the polar organic mode or stored in methanol.

The barium loading was estimated by the procedure described by Durmaz et al.<sup>37</sup> Briefly, untreated columns were conditioned with water and then methanol, 10-column volumes each. An HPLC method was developed where the column was washed with methanol at 0.5 mL/min for 5 min and then switched to a 5 mM  $\text{Ba}(\text{OAc})_2$  solution in methanol at 5.01 min at 0.5 mL/min. The method was continued until the breakthrough point (monitored at 204 and 210 nm) was observed. To regenerate the column, barium cations were eluted from the stationary phase using a 100 mM  $\text{NH}_4\text{OAc}$  solution (pH = 4.1) for 30 min. Barium elution was monitored until the effluent showed no sign of turbidity upon addition of a few drops of concentrated sodium sulfate solution.

## RESULTS AND DISCUSSION

While attempting to resolve enantiomers of CSA-5 by fractional recrystallization, simultaneous development of an HPLC method was undertaken to more accurately monitor the enantiomeric excess. Initially, a partial separation ( $R_s = 1.2$ ) was obtained on the LARIHC–CF6-P in the reversed-phase mode (see Figure 2A). This separation could not be optimized further, though different acidic and basic additives as well as ammonium salts were explored (not shown). Finally, knowing that cyclofructans bind barium ions strongly, 5 mM  $\text{Ba}(\text{OAc})_2$  was added to the mobile phase with the hope that it might induce better enantioselectivity for CSA-5. However the presence of this additive in the reversed-phase mode worsened

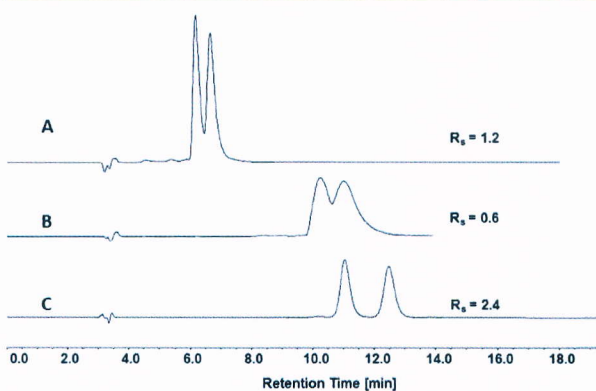


**Figure 2.** Original separation of CSA-5 on LARIHC–CF6-P. Mobile phase: (A) 80/20/0.1/0.1 (v/v %) water/MeOH/TEA/HOAc; (B) 5 mM  $\text{Ba}(\text{OAc})_2$  in 80/20 (v/v %) water/MeOH; (C) 50/50/0.1/0.1 ACN/MeOH/TEA/TFA; flow rate: 1 mL/min; detector: UV at 254 nm.

the selectivity and efficiency (see Figure 2B). When the normal phase was restored, 80/20/0.1 heptane/EtOH/TEA (not shown), CSA-5 was retained longer than before with strong peak tailing. Subsequently, the polar organic mode was used, and an excellent separation was obtained ( $R_s = 2.4$ ) with superior efficiency and peak shape compared to all other approaches (see Figure 2C). The separation was easily scaled to preparative amounts on the FRULIC-N (see Figure 3). When

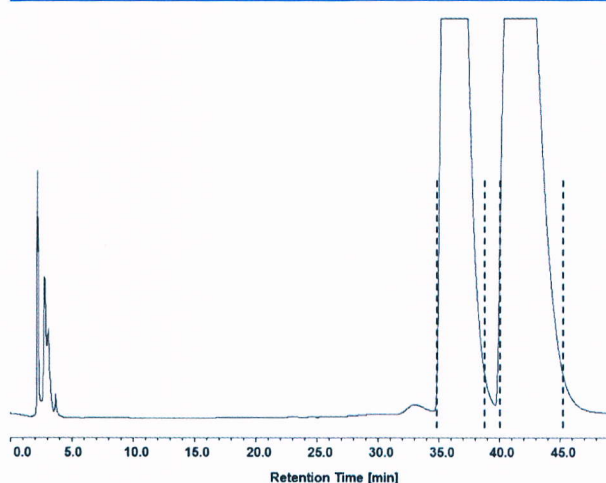


**Figure 3.** Preparative HPLC separation of racemic CSA-5 on 21.2 mm × 250 mm FRULIC-N treated with barium. Mobile phase: MeOH with 0.1/0.1 (v/v %) TEA/TFA; flow rate: 20 mL/min; UV: 280 nm; injection volume: 800  $\mu$ L; sample concentration: 48 mg/mL.

the barium is eluted from the stationary phase, there is no retention or enantioselectivity for CSA-5 enantiomers in the polar organic mode. When the column was reconditioned with a barium solution, retention and enantioselectivity were restored.

Table S-1 (see Supporting Information) shows the clear effect of barium treatment on the cyclofructan CSPs for all of the analytes in Figure 1. The untreated column was evaluated in the polar organic mode using methanol containing 10 mM  $\text{NH}_4\text{OAc}$ . Under these conditions, all analytes were eluted as sharp peaks close to the void volume with no enantioselectivity. If no additive was present in the mobile phase, analytes were still poorly retained but with poor peak efficiency. On a barium pretreated column and in the presence of a barium additive, however, there was a significant increase in retention often accompanied by an increase in enantioselectivity. Addition of low levels of barium salt to the mobile phase was necessary to maintain a constant level of barium on the stationary phase and to afford highly reproducible elution volumes and good peak efficiency. The order of retention strength for the three  $\text{Ba}^{2+}$ -doped columns, in this particular mobile phase, was FRULIC-N > LARIHC-CF6-RN > LARIHC-CF6-P. Retention is governed by (1) the loading of cyclofructan, which also dictates the amount of barium that can be loaded, (2) the nature of the selector, and (3) the nature of the analyte. The cyclofructan loading on the CSPs was determined to be 0.23, 0.12, and 0.18 mmol/g, respectively. Thus, even though the LARIHC-CF6-RN stationary phase had somewhat lower overall loading than the LARIHC-CF6-P, its ability to utilize  $\pi-\pi$  interactions with aromatic analytes resulted in greater overall retention in many cases.

**Effect of the Counteranion of the  $\text{Ba}^{2+}$  Salt.** The barium-doped stationary phases in this study can be treated as anion-exchange phases. However, to prevent slow leaching of the barium from the stationary phase and to maintain its level of saturation, a small amount of a barium salt is put into the mobile phase. Since a small amount of barium salt is in the mobile phase, the question arises as to the effect, if any, of its counteranion. It is known that retention in ion-exchange systems is believed to be a combination of selective adsorption, ion pairing, and accumulation in the diffuse layer.<sup>38</sup> As has already been shown (Table S-1), in the absence of barium

**Table 1. Comparison of Different Barium Salt Additives (~ 5 mM in Each Mobile Phase) on the Retention, Selectivity, and Resolution of Chiral Sulfonic/Phosphoric Acids on LARIHC-CF6-P in the Polar Organic Mode<sup>a</sup>**

analyte	5.0 mM $\text{Ba(OAc)}_2$ in MeOH			5.0 mM $\text{Ba(ClO}_4)_2$ in MeOH			5.0 mM $\text{Ba(MSA)}_2$ in MeOH			5.2 mM $\text{Ba(TFA)}_2$ in MeOH			5.2 mM $\text{Ba(TFA)}_2$ in EtOH		
	k	$\alpha$	$R_s$	k	$\alpha$	$R_s$	k	$\alpha$	$R_s$	k	$\alpha$	$R_s$	k	$\alpha$	$R_s$
CSA-1	0.57	1.00	<0.2	4.48	1.04	0.6	1.92	1.00	<0.4	2.89	1.03	0.4	3.94	1.06	0.6
CSA-2	0.57	1.00	<0.2	4.10	1.02	<0.5	1.76	1.00	<0.2	2.73	1.03	0.4	2.35	1.10	0.7
CSA-3	0.54	1.00	<0.2	4.18	1.00	<0.2	1.86	1.00	<0.2	2.82	1.00	<0.2	2.92	1.00	<0.2
CSA-4	0.90	1.00	<0.2	5.29	1.04	0.7	2.15	1.00	<0.4	3.30	1.03	0.4	4.11	1.06	0.6
CSA-5	0.68	1.11	1.0	4.86	1.28	4.2	2.06	1.16	2.4	3.20	1.21	3.3	2.91	1.22	1.8
CSA-6	0.76	1.07	0.4	3.68	1.24	1.8	1.46	1.12	1.3	2.29	1.15	1.9	2.79	1.25	1.6
CSA-7	0.71	1.00	<0.2	6.12	1.00	<0.2	2.34	1.00	<0.2	3.66	1.00	<0.2	6.28	1.00	<0.2
CSA-8	0.67	1.00	<0.2	5.55	1.00	<0.2	2.26	1.00	<0.2	3.42	1.00	<0.2	6.13	1.00	<0.2
CSA-9	0.66	1.00	<0.2	5.42	1.03	0.5	2.35	1.00	0.4	3.37	1.02	0.4	6.91	1.04	0.5
CPA-1	0.58	1.09	0.7	2.35	1.24	3.4	1.56	1.11	1.5	1.95	1.16	2.3	2.16	1.37	3.1
CPA-2	0.91	1.00	<0.2	8.40	1.03	0.5	3.04	1.00	<0.2	4.84	1.00	<0.4	8.44	1.09	1.1
CPA-3	0.38	1.00	<0.2	1.69	1.00	<0.2	1.53	1.00	<0.2	1.70	1.00	<0.2	2.23	1.18	2.0
CPA-4	0.20	1.00	<0.2	1.00	1.05	0.6	0.92	1.00	<0.2	1.02	1.00	<0.4	2.25	1.19	2.8
CPA-5	1.21	1.00	<0.2	15.95	1.03	<0.4	3.96	1.03	0.5	7.18	1.04	0.6	11.64	1.08	0.6
CPA-6	1.08	1.00	<0.2	12.93	1.02	<0.4	3.59	1.00	<0.2	6.32	1.00	<0.2	10.83	1.00	<0.2
CPA-7	0.28	1.00	<0.2	1.65	1.00	<0.2	1.27	1.00	<0.2	1.47	1.00	<0.2	2.83	1.10	1.4

<sup>a</sup>Mobile phase: methanol (or ethanol) with 5 mM  $\text{BaX}_2$  where X = acetate ( $\text{OAc}^-$ ), perchlorate ( $\text{ClO}_4^-$ ), methane sulfonate ( $\text{MSA}^-$ ), and trifluoroacetate ( $\text{TFA}^-$ ).

cations, analytes elute at the dead volume or are poorly retained on these stationary phases in the polar organic mode. However, they are retained on the same stationary phases that have been doped with barium. The effect of three other barium salts (methanesulfonate, perchlorate, and trifluoroacetate) on retention and enantioselectivity was explored using the LARIHC-CF6-P column (Table 1). It is clear that the order of elution strength for the four counteranions is:  $\text{OAc}^- > \text{MSA}^- > \text{TFA}^- > \text{ClO}_4^-$ . As retention increases, the number of analytes that show selectivity ( $R_s > 0.4$ ) also increases as follows: 11 compounds for  $\text{ClO}_4^-$ , 8 compounds for  $\text{TFA}^-$ , 4 compounds for  $\text{MSA}^-$ , and 3 compounds for  $\text{OAc}^-$ . However, the observed enantioselectivities are not simply a function of retention. Figure 4 shows the separation of CSA-5 and CPA-1.

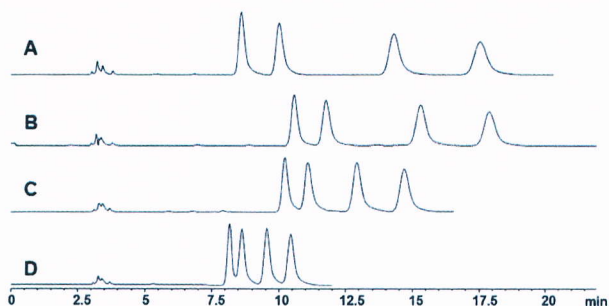


**Figure 4.** Overlay of four chromatograms on LARIHC-CF6-P. In each case, the first pair of enantiomers corresponds to CPA-1 and the latter to CSA-5; flow rate: 1 mL/min, UV = 230 nm. Mobile phase conditions and enantioselectivity: (A) 5.11 mM  $\text{Ba}(\text{ClO}_4)_2$  in methanol,  $\alpha_{\text{CPA-1}} = 1.25$ ,  $\alpha_{\text{CSA-5}} = 1.29$ ; (B) 4.16 mM  $\text{Ba}(\text{TFA})_2$  in methanol,  $\alpha_{\text{CPA-1}} = 1.16$ ,  $\alpha_{\text{CSA-5}} = 1.21$ ; (C) 2.00 mM  $\text{Ba}(\text{MSA})_2$  in methanol,  $\alpha_{\text{CPA-1}} = 1.12$ ,  $\alpha_{\text{CSA-5}} = 1.18$ ; (D) 1.00 mM  $\text{Ba}(\text{OAc})_2$  in methanol,  $\alpha_{\text{CPA-1}} = 1.09$ ,  $\alpha_{\text{CSA-5}} = 1.12$ .

using the four different barium salts at concentrations that afford similar retention.  $\text{ClO}_4^-$  has a profound effect on the enantioselectivity for these two compounds that is clearly greater than  $\text{TFA}^-$ ,  $\text{MSA}^-$ , and  $\text{OAc}^-$ .

Moyer et al. used the phrase “Hofmeister effect or bias” in their research on cesium extraction by crown ethers.<sup>39</sup> The phrase was used to describe the observation that in liquid–liquid extraction systems, the partitioning of cesium improved when chaotropic counteranions were present. It appears that there are analogous effects or trends in these chromatographic results. The well-known Hofmeister series ranks the counteranions used in this publication as:  $\text{OAc}^- > \text{MSA}^- > \text{TFA}^- > \text{ClO}_4^-$  with  $\text{OAc}^-$  being the most kosmotropic (water structure or hydrogen bond making) and  $\text{ClO}_4^-$  the most chaotropic (water structure or hydrogen bond breaking).<sup>39,40</sup> While these terms, water structure making or breaking, may seem to have no direct bearing on the polar organic mobile phase used here, other recent publications have indicated Hofmeister effects in nonaqueous solvents or aqueous organic mixtures.<sup>41,42</sup> Indeed, the current trend for explaining the Hofmeister series for anions is not in terms of their effect on bulk water structure but rather their direct interaction with the interface of the substrate.<sup>43</sup>

We postulate that kosmotropic anions, such as acetate, will have a tendency to selectively adsorb to cyclofructan through its many hydroxyl groups. The effect of such a selective adsorption is illustrated in Scheme 1. The original surface potential of the barium-complexed cyclofructan,  $\psi_0$ , is lowered to a new surface

potential,  $\psi_{0,\text{Ads}}$ , by the adsorption of acetate anions to the cyclofructan macrocycle resulting in decreased retention of analytes. In extreme cases, this selective adsorption can lead to a reversal of the surface potential.<sup>38</sup> Interestingly, this behavior was observed when oxalic acid/TEA and phosphoric acid/TEA were evaluated as mobile phase additives with no barium present in the mobile phase. The result (data not shown) was that chiral phosphoric and sulfonic acids eluted at the void volume (exclusion) and racemic 1-(1-naphthyl)ethylamine was retained and separated! Selective adsorption to the stationary phase particle will lessen as the nature of the anion becomes more chaotropic as with perchlorate.

**Effect of the Mobile Phase Dielectric Constant.** Also in Table 1, we note the important role that the dielectric constant of the solvent plays. Methanol has a dielectric constant of 32.7, and ethanol has a value of 24.5. The replacement of methanol for ethanol in Table 1, while using the same additive, 5.2 mM  $\text{Ba}(\text{TFA})_2$ , shows (i) an increase in retention for every compound except CSA-2 and CSA-5, (ii) an improvement in the enantioselectivity, and (iii) additional enantioselectivity that did not occur in the methanol mobile phase (CPA-2–4 and 7). The number of compounds exhibiting enantioselectivity when changing from methanol to ethanol is improved from 8 to 12, respectively. The rationale for these improvements is that a lower solvent dielectric constant affords tighter ion pairing with the barium cation and therefore longer retention. Tighter ion pairing necessitates being closer to the chiral macrocycle, thus enhancing enantioselectivity as well. Although ethanol was the preferable polar organic solvent, the kosmotropic barium salts ( $\text{OAc}^-$  and  $\text{MSA}^-$ ) were insoluble in it. The use of even lower dielectric constant systems was investigated for poorly retained compounds such as CPA-3 and CPA-4 by using heptane–ethanol mobile phases. This improved both the retention and the enantioselectivity; however, it caused excessive retention of the other analytes.

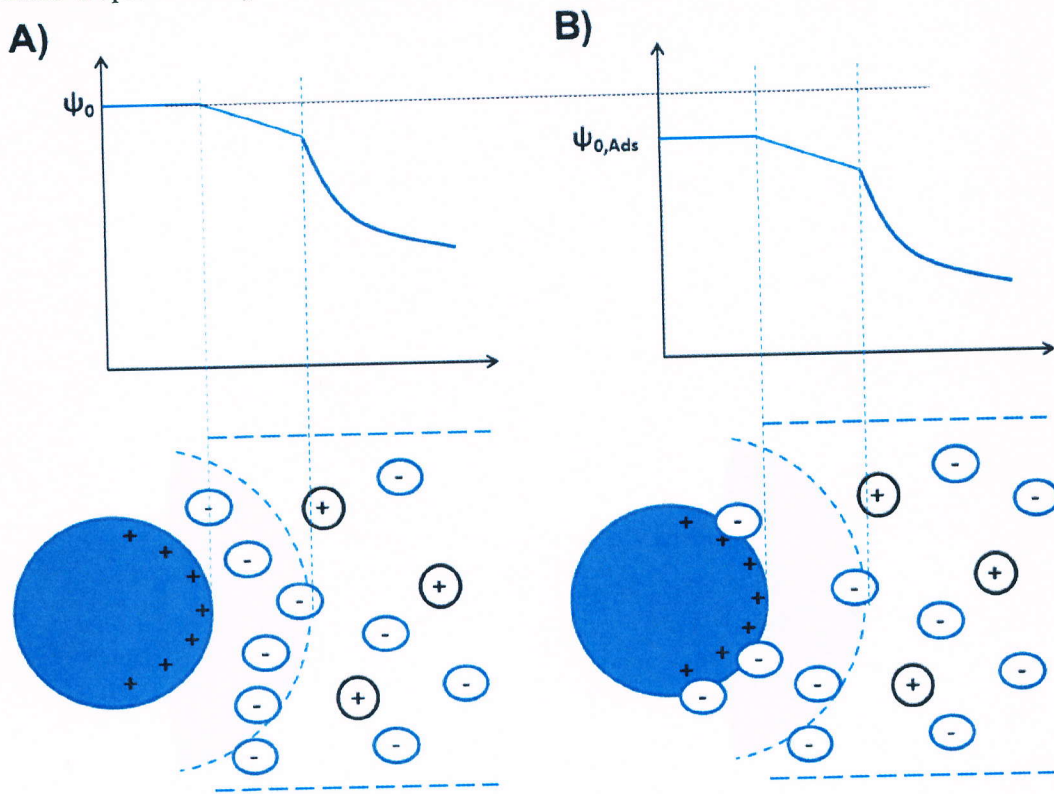
**Retention Order.** In methanol mobile phases containing  $\text{MSA}^-$ ,  $\text{TFA}^-$ , and  $\text{ClO}_4^-$  (Table 1), the retention order on LARIHC-CF6-P appeared to follow the geometry and accessibility of the anionic moiety. The more sterically hindered the ionizable group of the analyte was, the less it was retained. The most retained compounds, CPA-2, CPA-5, and CPA-6, are among the smallest and least sterically hindered of the CPAs, and they are retained the longest. Conversely, the largest analytes (CPA-3, CPA-4, and CPA-7) are the least retained, presumably because of the steric hindrance of the phosphate group.

**Effect of Varying Concentration of the  $\text{Ba}^{2+}$  Salt in the Mobile Phase.** The retention of CPA-1 and CSA-5 was studied as a function of the barium salt concentration by systematically changing it from 1–5 mM for each of the barium salts (~1.0, 2.0, 3.0, 4.0, and 5.0 mM). Plots of the logarithm of the retention factor for the first eluting enantiomer ( $\log k$ ) versus the logarithm of the concentration of the counteranion of the barium salt ( $\log [X]$ , where  $X$  = the barium salt counteranion,  $\text{OAc}^-$ ,  $\text{MSA}^-$ ,  $\text{TFA}^-$ , and  $\text{ClO}_4^-$ ) were all linear ( $r^2 > 0.99$ ) according to the equation

$$\log k = -s \log [X] + \text{constant} \quad (1)$$

where  $k$  is the retention factor,  $s$  is the slope which is usually found to be approximately equal to  $z_A/z_X$  where  $z_A$  is the charge of the analyte anion and  $z_X$  is the charge of the barium counteranion. The negative slopes (see Table S-2) indicated a decreasing retention time with increasing barium salt

Scheme 1. Effect of Specific Adsorption of Eluent Anions on the Potential Curve of a Charged Surface<sup>a</sup>



<sup>a</sup>The blue sphere represents a charged object or particle. The shaded, hemispherical area with dashed boundary is the Stern layer. The ovoid shapes with a negative charge indicate eluent anions, and the spheres containing a positive charge indicate cations. The boundary to the diffuse layer is not shown. (A) No selective adsorption of anions to the charged surface, potential is  $\psi_0$ . (B) Selective adsorption of anion to the charged surface,  $\psi_{0,Ads} < \psi_0$ .

concentration typical of that found in ion-exchange chromatography.<sup>33,38,44</sup> In classical ion-pairing techniques, analyte retention initially increases with increasing concentration of ion-pairing reagent up to a maximum and thereafter decreases. Assuming linear behavior, a positive slope for log  $k$  versus log [X] should be seen for the former case and a negative one for the latter. At greater barium salt concentrations, where solubility permitted (e.g., 100 mM Ba(ClO<sub>4</sub>)<sub>2</sub>), retention continued to decrease. When the concentration of the barium salt in the mobile phase is much greater than that on the stationary phase, the analytes predominantly ion pair in the mobile phase and are not retained. Retention can then be increased by decreasing the barium salt concentration to afford separation.

Lamb et al. have shown in their work on C18 reversed phase columns coated with a lipophilic crown ether/cryptand using a KOH hydro-organic mobile phase that below ~0.8 mM KOH, retention increased with increasing KOH concentration, but thereafter it decreased linearly.<sup>45</sup> Such a turning point must exist for our stationary phase as well but we did not observe it. Fritz has observed that some ion-pairing agents can be attached so strongly to the stationary phase that they may be considered as permanently coated.<sup>46</sup> In our case, this seems to have some merit because the binding of Ba<sup>2+</sup> to cyclofructan is stronger in a pure organic solvent as is also common for crown ethers in general.<sup>29,47</sup>

**van't Hoff Plots.** Before delving into the thermodynamics of the chromatography, the thermodynamics of the barium-

cyclofructan complex must be addressed. As with the binding of alkali and alkaline earth metals to synthetic crown ethers and cryptands, the binding of barium to cyclofructan is an exothermic process.<sup>47–50</sup> Although there is no quantitative thermodynamic data on the binding of barium to cyclofructan, it is nevertheless undisputed that it binds strongest to cyclofructan compared to the rest of the Group I and II metal cations.<sup>29</sup> Takai and Sewada have generated thermodynamic data for the binding of potassium, rubidium, and cesium cations to permethylated cyclofructan and have shown that  $\Delta H_{\text{binding}}$  becomes increasingly exothermic.<sup>15</sup> We therefore infer that an analogous enthalpy will be exhibited for barium binding to cyclofructan derivatives. A question arises as to how much barium will be decomplexed from the cyclofructan macrocycle as the equilibrium shifts to dissociation with increasing temperature. The van't Hoff equation expresses the changing equilibrium constant as a function of temperature as follows<sup>48</sup>

$$\ln \frac{K_2}{K_1} = \frac{-\Delta H}{R} \left( \frac{1}{T_2} - \frac{1}{T_1} \right) \quad (2)$$

where  $K_1$  and  $K_2$  represent the equilibrium constants at absolute temperatures  $T_1$  and  $T_2$ , respectively,  $\Delta H$  is the change in enthalpy (in J·mol<sup>-1</sup>), and  $R$  is the gas constant (8.314 J·K<sup>-1</sup>·mol<sup>-1</sup>). Thus, if  $\Delta H$ ,  $K_1$ , and  $T_1$  are known, the equilibrium constant,  $K_2$ , at some other temperature,  $T_2$ , can be readily calculated. Furthermore, the ratio of Ba<sup>2+</sup>–CF6 complex

on the stationary phase to uncomplexed CF6 on the stationary phase may be expressed as follows<sup>45</sup>

$$\frac{[\text{Ba}^{2+}\cdots\text{CF6}]_{\text{S.P.}}}{[\text{CF6}]_{\text{S.P.}}} = K[\text{Ba}^{2+}]_{\text{M.P.}} \quad (3)$$

where  $K$  is the equilibrium constant,  $[\text{Ba}^{2+}]_{\text{M.P.}}$  represents the concentration of barium in the mobile phase,  $[\text{Ba}^{2+}\cdots\text{CF6}]_{\text{S.P.}}$  represents the concentration of the barium–CF6 complex on the stationary phase, and  $[\text{CF6}]_{\text{S.P.}}$  represents the concentration of CF6 on the stationary phase. We chose a  $K$  value for  $\text{Ba}^{2+}$ –CF6 of  $19\,000\text{ M}^{-1}$  taken from Takai and Sewada et al.,<sup>15,16</sup> which is in agreement with research done by Na and Padivitge.<sup>29</sup> For  $\Delta H$ , we used the value reported by Takai and Sewada for cesium complexed to permethylated CF6<sup>15</sup> (i.e.,  $\Delta H = -38\text{ kJ}\cdot\text{mol}^{-1}$ ). The calculations for eqs 2 and 3 are represented graphically in Figure 5. The net decrease in the

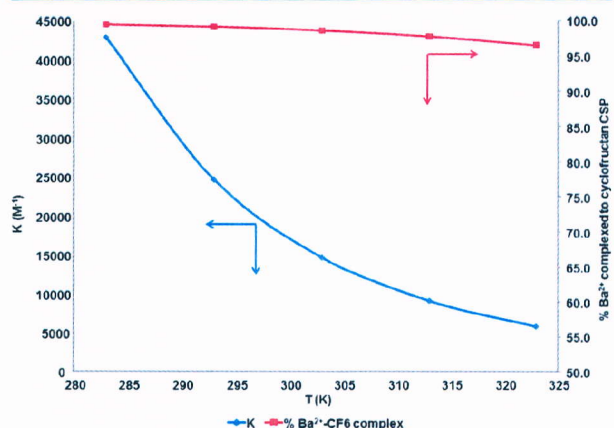


Figure 5. Change of  $K$  (blue diamond) as a function of temperature overlaid with the change in the %  $\text{Ba}^{2+}$ –CF6 complexes (red square).

amount of barium on the CSP over the temperature range studied is estimated to be  $\sim 3.5\%$  or in other words, 96.5% of the barium remains on the CSP. This very small change in the  $\text{Ba}^{2+}$  concentration with increasing temperature is not expected to have a significant impact on retention.

$\ln k$  vs  $1000/T$

The retention and enantioselectivity of CPA-1 and CSA-5 on LARIHC–CF6-P were monitored as a function of mobile phase temperature according to the well-known van't Hoff expressions for chromatography

$$\ln k = -\frac{\Delta H}{RT} + \frac{\Delta S}{R} + \ln \phi \quad (4)$$

$$\ln \alpha = -\frac{\Delta \Delta H}{RT} + \frac{\Delta \Delta S}{R} \quad (5)$$

where  $k$  is the retention factor,  $\Delta H$  is the change in enthalpy,  $\Delta S$  is the change in entropy,  $R$  is the gas constant ( $8.314\text{ J}\cdot\text{K}^{-1}\cdot\text{mol}^{-1}$ ),  $T$  is the absolute temperature,  $\phi$  is the phase ratio ( $V_s/V_m$  where  $V_s$  is the volume of the selector (i.e., excluding the silica support material) and  $V_m$  is the volume of the mobile phase), and  $\alpha$  is enantioselectivity. The thermodynamic parameters calculated from the van't Hoff plots (see Figures S-1–S-4 in Supporting Information) of CPA-1 and CSA-5 are shown in Table 2. The  $\ln k$  versus  $1000/T$  van't Hoff plot governs the thermodynamics of retention as the analyte moves from the mobile phase to the stationary phase. Here, we observed two extremes:  $\text{Ba}(\text{ClO}_4)_2$  was an enthalpy driven system ( $\Delta H < 0$  and  $\Delta H < T\Delta S$ ), while  $\text{Ba}(\text{OAc})_2$  was purely entropy driven ( $\Delta H > 0$  and  $\Delta H < T\Delta S$ ).  $\text{Ba}(\text{TFA})_2$  was an intermediate between these two extremes in that although  $\Delta H < 0$ , the  $\Delta G$  was dominated by the  $T\Delta S$  contribution.

The solvation of the cyclofructan macrocycle, the barium cation, and the analyte should be more or less constant in each mobile phase system. Furthermore, the number of barium counteranions that undergo ionic interactions with the complexed barium should also be constant. The remaining variable is the nature of the anion and its ability to associate with the stationary phase via hydrogen bonding. We postulate that analyte retention is governed both by ionic interaction as well as hydrogen bonding. The former interaction will be present in both  $\text{OAc}^-$  and  $\text{ClO}_4^-$  mobile phase systems; however, the latter interaction will be unfavorable for the strongly hydrogen bonded  $\text{OAc}^-$  system and absent in the  $\text{ClO}_4^-$  system. The removal of tightly hydrogen bonded  $\text{OAc}^-$  anions from the stationary phase to the mobile phase affords an increase in its degrees of freedom and a consequent increase in entropy.

$\ln \alpha$  vs  $1000/T$

Table 2. Thermodynamic Parameters Calculated from the van't Hoff Plots in Figures S-1–S-4 (See Supporting Information)

		$\ln(k)$ vs $1000/T$			$\ln(\alpha)$ vs $1000/T$		
		$\Delta H$ ( $\text{kJ}\cdot\text{mol}^{-1}$ )	$\Delta S$ ( $\text{J}\cdot\text{K}^{-1}\cdot\text{mol}^{-1}$ )	$\Delta G_{298\text{ K}}$ ( $\text{kJ}\cdot\text{mol}^{-1}$ )	$\Delta \Delta H$ ( $\text{kJ}\cdot\text{mol}^{-1}$ )	$\Delta \Delta S$ ( $\text{J}\cdot\text{K}^{-1}\cdot\text{mol}^{-1}$ )	$\Delta \Delta G_{298\text{ K}}$ ( $\text{kJ}\cdot\text{mol}^{-1}$ )
5.2 mM $\text{Ba}(\text{TFA})_2$	1 <sup>st</sup> enantiomer	-2.06	15.30	-6.62	0.28	2.20	-0.38
	2 <sup>nd</sup> enantiomer	-1.78	17.50	-7.00			
CSA-5	1 <sup>st</sup> enantiomer	-3.29	15.28	-7.85	-0.78	-0.95	-0.49
	2 <sup>nd</sup> enantiomer	-4.07	14.33	-8.34			
5.11 mM $\text{Ba}(\text{ClO}_4)_2$							
CPA-1	1 <sup>st</sup> enantiomer	-5.59	2.50	-6.34	0.51	3.57	-0.55
	2 <sup>nd</sup> enantiomer	-5.08	6.07	-6.89			
CSA-5	1 <sup>st</sup> enantiomer	-6.76	4.44	-8.08	-0.87	-0.83	-0.63
	2 <sup>nd</sup> enantiomer	-7.63	3.61	-8.71			
1.01 mM $\text{Ba}(\text{OAc})_2$							
CPA-1	1 <sup>st</sup> enantiomer	3.07	31.27	-6.86	0.19	1.38	-0.23
	2 <sup>nd</sup> enantiomer	3.26	32.65	-7.20			
CSA-5	1 <sup>st</sup> enantiomer	3.28	34.04	-6.24	-0.63	-1.01	-0.33
	2 <sup>nd</sup> enantiomer	2.65	33.03	-6.47			

**Table 3.** Optimized Separations of Chiral Sulfonic/Phosphoric Acids on Cyclofructan Columns<sup>a</sup>

analyte	column	mobile phase	$k_1$	$\alpha$	$R_s$
CSA-1	LARIHC-CF6-RN	EtOH with 0.05/0.05 (v/v %) TEA/TFA and 0.5 mM Ba(TFA) <sub>2</sub>	17.49	1.04	0.7
CSA-2	LARIHC-CF6-RN	EtOH with 0.05/0.05 (v/v %) TEA/TFA and 0.5 mM Ba(TFA) <sub>2</sub>	11.86	1.09	1.5
CSA-3	LARIHC-CF6-RN	EtOH with 0.08/0.02 (v/v %) TEA/TFA and 1.0 mM Ba(TFA) <sub>2</sub>	7.22	1.12	1.9
CSA-4	LARIHC-CF6-RN	EtOH with 0.05/0.05 (v/v %) TEA/TFA and 0.5 mM Ba(TFA) <sub>2</sub>	19.59	1.06	1.1
CSA-5	LARIHC-CF6-P	MeOH with 5 mM Ba(ClO <sub>4</sub> ) <sub>2</sub>	4.86	1.28	4.2
CSA-6	LARIHC-CF6-RN	MeOH with 5 mM Ba(ClO <sub>4</sub> ) <sub>2</sub>	3.68	1.24	1.8
CSA-7	LARIHC-CF6-RN	EtOH with 0.1/0.1 (v/v %) TEA/TFA and 1 mM Ba(TFA) <sub>2</sub>	13.88	1.05	1.0
CSA-8	FRULIC-N	MeOH with 5 mM Ba(TFA) <sub>2</sub>	26.49	1.04	1.0
CSA-9	FRULIC-N	MeOH with 5 mM Ba(TFA) <sub>2</sub>	27.94	1.06	1.3
CPA-1	LARIHC-CF6-RN	MeOH with 5 mM Ba(TFA) <sub>2</sub>	4.01	1.23	4.4
CPA-2	LARIHC-CF6-RN	EtOH with 5 mM Ba(ClO <sub>4</sub> ) <sub>2</sub>	13.90	1.23	2.2
CPA-3	LARIHC-CF6-RN	EtOH with 5.2 mM Ba(TFA) <sub>2</sub>	4.95	1.14	1.7
CPA-4	LARIHC-CF6-RN	EtOH with 5.2 mM Ba(TFA) <sub>2</sub>	3.01	1.27	4.2
CPA-5	LARIHC-CF6-RN	MeOH with 1 mM Ba(OAc) <sub>2</sub>	12.10	1.06	1.6
CPA-6	LARIHC-CF6-RN	MeOH with 1 mM Ba(OAc) <sub>2</sub>	10.86	1.05	1.5
CPA-7	LARIHC-CF6-P	EtOH with 5.2 mM Ba(TFA) <sub>2</sub> *	6.78	1.08	1.8

<sup>a</sup>In all cases, the flow rate was set to 1 mL/min, except for \*, where it was set at 0.5 mL/min.

With regard to the Gibbs free energy (Table 2) for the enantioselectivity, we once again observed two extreme cases: Ba(ClO<sub>4</sub>)<sub>2</sub> exhibits the most favorable  $\Delta\Delta G$  ( $-0.55$  and  $-0.63$  kJ·mol<sup>-1</sup> for CPA-1 and CSA-5, respectively), while Ba(OAc)<sub>2</sub>, though still favorable, exhibits the smallest  $\Delta\Delta G$  ( $-0.23$  and  $-0.33$  kJ·mol<sup>-1</sup> for CPA-1 and CSA-5, respectively). Ba(TFA)<sub>2</sub> is once again intermediate between the two extremes ( $-0.38$  and  $-0.49$  kJ·mol<sup>-1</sup> for CPA-1 and CSA-5, respectively). A possible explanation for the poor enantioselectivity observed in the Ba(OAc)<sub>2</sub> system is that adsorbed acetate anions would impede hydrogen bonding interactions between the analyte and the chiral selector. Three points of interaction are required for chiral recognition,<sup>51</sup> and one of these is ionic. The remaining interactions can be hydrogen bonding, dipole–dipole, and/or steric interactions. In the case of Ba(ClO<sub>4</sub>)<sub>2</sub>, though, the analyte would be free to hydrogen bond and would therefore exhibit better chiral recognition, which was observed.

The data in Table 2 demonstrate that the enantiomeric separation of CPA-1 is entropically driven, while CSA-5 is enthalpically driven for each mobile phase system. This means, in the case of Ba(ClO<sub>4</sub>)<sub>2</sub> and Ba(TFA)<sub>2</sub> systems, that as temperature is increased, enantioselectivity for CPA-1 improves even while retention is decreasing (see Figure S-5 in the Supporting Information). Such remarkable enantioselective behavior is rarely observed. Since it is unlikely that the cyclofructan macrocycle is changing and since the thermodynamic behavior for each analyte is consistent regardless of the barium additive used, the observed behavior must be related to the analyte structure. Both CPA-1 and CSA-5 are sterically hindered molecules; however, the sulfonate group has some rotational degree of freedom, whereas the phosphate group does not.

**Optimized Separations.** Table 3 shows the optimized separations for all the analytes in Figure 1. For the  $\beta$ -ketosulfonic acids (CSA-7–9), the LARIHC-CF6-RN and the FRULIC-N showed complementary behavior. CSA-7, chalcone sulfonic acid containing no aromatic substituents, displayed enantioselectivity on the LARIHC-CF6-RN column, whereas the para-substituted CSA-8 and CSA-9 showed no selectivity. Evidently, the presence of a para substituent was unfavorable for enantioselectivity. The FRULIC-N showed reasonable enantioselectivity for CSA-8 and CSA-9 but only slight

enantioselectivity for CSA-7. In fact, the FRULIC-N was the only CSP to show appreciable selectivity for these two compounds. Single chiral axis sulfonic acids (CSA-1 and CSA-4) displayed longer retention but smaller enantioselectivity than the two chiral axes analogues (CSA-3 and CSA-5). Figure S-6 in the Supporting Information shows the overall performance of the three CSPs in separating chiral sulfonic and phosphoric acids (Figure 1). The LARIHC-CF6-RN was clearly the most successful in terms of the number of baseline separations. It displayed enantioselectivity for every analyte except CSA-9, which was best separated on the FRULIC-N.

## CONCLUSIONS

The selectivity of cyclofructan-based CSPs has been significantly expanded to an entirely new class of anionic compounds. Preliminary tests for carboxylates are also promising. This has been achieved by exploiting a unique ion-pairing behavior of a simple inorganic metal ion (Ba<sup>2+</sup>). Once the CSPs have been conditioned and evaluated in the polar organic mode (methanol or ethanol) with a barium salt in the mobile phase, log  $k$  vs log [X] plots are linear with negative slopes and behave as anion exchangers. Sterically hindered sulfonates or phosphates elute earlier than the less sterically hindered ones. The presence of additional hydrogen bond acceptors on the analyte also increases retention. Ba(OAc)<sub>2</sub> mobile phase additive affords shorter retention, which for CPA-1 and CSA-5, is entropy driven, while Ba(ClO<sub>4</sub>)<sub>2</sub> affords longer retention, which is enthalpy driven and Ba(TFA)<sub>2</sub> is intermediate. Enantioselectivity improves in the order of OAc<sup>-</sup> < TFA<sup>-</sup> < ClO<sub>4</sub><sup>-</sup>. The scale up of a separation of CSA-5 to preparative scale LC has also been successfully demonstrated. Barium-complexed cyclofructans behave as hydrophilic analogues of reversed-phase ion-pairing LC systems.

## ASSOCIATED CONTENT

### Supporting Information

Additional information as noted in the text. This material is available free of charge via the Internet at <http://pubs.acs.org>.

## AUTHOR INFORMATION

### Corresponding Author

\*E-mail: sec4dwa@uta.edu.

## Notes

The authors declare no competing financial interest.

## ACKNOWLEDGMENTS

We gratefully acknowledge the Welch Foundation (Y-0026) for their continued support. The Krische group gratefully acknowledges the Shanghai Institute of Organic Chemistry (SIOC) Postdoctoral Fellowship and the Welch Foundation (F-0038).

## REFERENCES

- (1) Akiyama, T.; Itoh, J.; Yokota, K.; Fuchibe, K. *Angew. Chem., Int. Ed.* **2004**, *43*, 1566–1568.
- (2) Uraguchi, D.; Sorimachi, K.; Terada, M. *J. Am. Chem. Soc.* **2004**, *126*, 11804–11805.
- (3) Terada, M. *Chem. Commun.* **2008**, 4097–4112.
- (4) Li, G.-Q.; Gao, H.; Keene, C.; Devonas, M.; Ess, D. H.; Kurti, L. *J. Am. Chem. Soc.* **2013**, *135*, 7414–7417.
- (5) Sun, Z.; Winschel, G. A.; Borovka, A.; Nagorny, P. *J. Am. Chem. Soc.* **2012**, *134*, 8074–8077.
- (6) Zhang, H.; Wen, X.; Gan, L.; Peng, Y. *Org. Lett.* **2012**, *14*, 2126–2129.
- (7) Zamfir, A.; Tsogoeva, S. B. *Org. Lett.* **2010**, *12*, 188–191.
- (8) Storer, R. I.; Carrera, D. E.; Ni, Y.; MacMillan, D. W. C. *J. Am. Chem. Soc.* **2006**, *128*, 84–86.
- (9) McInturff, E. L.; Yamaguchi, E.; Krische, M. J. *J. Am. Chem. Soc.* **2012**, *134*, 20628–20631.
- (10) Zbieg, J. R.; Yamaguchi, E.; McInturff, E. L.; Krische, M. J. *Science* **2012**, *336*, 324–327.
- (11) Kellogg, R. M.; Nieuwenhuijzen, J. W.; Pouwer, K.; Vries, T. R.; Broxterman, Q. B.; Grimborgen, R. F. P.; Kaptein, B.; La Crois, R. M.; de Weer, E.; Zwaagstra, K.; van der Laan, A. C. *Synthesis* **2003**, 1626–1638.
- (12) Loh, J. S. C.; van Enckevort, W. J. P.; Vlieg, E.; Gervais, C.; Grimborgen, R. F. P.; Kaptein, B. *Cryst. Growth Des.* **2006**, *6*, 861–865.
- (13) Bathori, N. B.; Nassimbeni, L. R. *Cryst. Growth Des.* **2012**, *12*, 2501–2507.
- (14) Kawamura, M.; Uchiyama, T.; Kuramoto, T.; Tamura, Y.; Mizutani, K. *Carbohydr. Res.* **1989**, *192*, 83–90.
- (15) Shizuma, M.; Takai, Y.; Kawamura, M.; Takeda, T.; Sawada, M. *J. Chem. Soc., Perkin Trans. 2* **2001**, 1306–1314.
- (16) Takai, Y.; Okumura, Y.; Tanaka, T.; Sawada, M.; Takahashi, S.; Shiro, M.; Kawamura, M.; Uchiyama, T. *J. Org. Chem.* **1994**, *59*, 2967–2975.
- (17) Uchiyama, T.; Kawamura, M.; Uragami, T.; Okuno, H. *Carbohydr. Res.* **1993**, *241*, 245–248.
- (18) Yoshie, N.; Hamada, H.; Takada, S.; Inoue, Y. *Chem. Lett.* **1993**, *2*, 353–356.
- (19) Sun, P.; Wang, C.-L.; Breitbach, Z. S.; Zhang, Y.; Armstrong, D. W. *Anal. Chem.* **2009**, *81*, 10215–10226.
- (20) Aranyi, A.; Bagi, A.; Ilysz, I.; Pataj, Z.; Fueloep, F.; Armstrong, D. W.; Peter, A. *J. Sep. Sci.* **2012**, *35*, 617–624.
- (21) Gondova, T.; Petrovaj, J.; Kutschy, P.; Armstrong, D. W. *J. Chromatogr. A* **2013**, *1272*, 100–105.
- (22) Kozlik, P.; Simova, V.; Kalikova, K.; Bosakova, Z.; Armstrong, D. W.; Tesarova, E. *J. Chromatogr. A* **2012**, *1257*, 58–65.
- (23) Padivituge, N. L. T.; Armstrong, D. W. *J. Sep. Sci.* **2011**, *34*, 1636–1647.
- (24) Padivituge, N. L. T.; Dissanayake, M. K.; Armstrong, D. W. *Anal. Bioanal. Chem.* **2014**, *405*, 8837–8848.
- (25) Qiu, H.; Loukotkova, L.; Sun, P.; Tesarova, E.; Bosakova, Z.; Armstrong, D. W. *J. Chromatogr. A* **2011**, *1218*, 270–279.
- (26) Sun, P.; Armstrong, D. W. *J. Chromatogr. A* **2010**, *1217*, 4904–4918.
- (27) Sun, P.; Wang, C.; Padivituge, N. L. T.; Nanayakkara, Y. S.; Perera, S.; Qiu, H.; Zhang, Y.; Armstrong, D. W. *Analyst* **2011**, *136*, 787–800.
- (28) Vozka, J.; Kalikova, K.; Roussel, C.; Armstrong, D. W.; Tesarova, E. *J. Sep. Sci.* **2013**, *36*, 1711–1719.
- (29) Na, Y.-C. P.; Nilusha, L. T.; Dissanayake, M. K.; Armstrong, D. W. *Supramol. Chem.* **2014**, DOI: 10.1080/10610278.2013.85.
- (30) Rogozhin, S. V.; Davankov, V. A. *J. Chem. Soc. D* **1971**, 490a–.
- (31) Roumeliotis, P.; Unger, K. K.; Kurganov, A. A.; Davankov, V. A. *J. Chromatogr. A* **1983**, *255*, 51–66.
- (32) Bidlingmeyer, B. A.; Deming, S. N.; Price, W. P., Jr.; Sachok, B.; Petrusk, M. *J. Chromatogr. A* **1979**, *186*, 419–434.
- (33) Pell, R.; Schuster, G.; Laemmerhofer, M.; Lindner, W. *J. Sep. Sci.* **2012**, *35*, 2521–2528.
- (34) Gargano, A. F. G.; Kohout, M.; Macikova, P.; Laemmerhofer, M.; Lindner, W. *Anal. Bioanal. Chem.* **2013**, *405*, 8027–8038.
- (35) Qiu, H.; Armstrong, D. W.; Berthod, A. *J. Chromatogr. A* **2013**, *1272*, 81–89.
- (36) Gritt, F.; Guiochon, G. *Anal. Chem.* **2006**, *78*, 4642–4653.
- (37) Durmaz, F.; Memon, F. N.; Memon, N. A.; Memon, S.; Memon, S.; Kara, H. *Chromatographia* **2013**, *76*, 909–919.
- (38) Okada, T. *Anal. Chem.* **1998**, *70*, 1692–1700.
- (39) Levitskaia, T. G.; Maya, L.; Van Berk, G. J.; Moyer, B. A. *Inorg. Chem.* **2006**, *46*, 261–272.
- (40) Roberts, J. M.; Diaz, A. R.; Fortin, D. T.; Friedle, J. M.; Piper, S. D. *Anal. Chem.* **2002**, *74*, 4927–4932.
- (41) Peruzzi, N.; Ninham, B. W.; Lo, N. P.; Baglioni, P. *J. Phys. Chem. B* **2012**, *116*, 14398–14405.
- (42) Bilaničová, D.; Salis, A.; Ninham, B. W.; Monduzzi, M. *J. Phys. Chem. B* **2008**, *112*, 12066–12072.
- (43) Zhang, Y.; Cremer, P. S. *Curr. Opin. Chem. Biol.* **2006**, *10*, 658–663.
- (44) Staahlberg, J. *Anal. Chem.* **1994**, *66*, 440–449.
- (45) Lamb, J. D.; Drake, P. A. *J. Chromatogr.* **1989**, *482*, 367–380.
- (46) Fritz, J. S. *J. Chromatogr. A* **2005**, *1085*, 8–17.
- (47) Izatt, R. M.; Bradshaw, J. S.; Nielsen, S. A.; Lamb, J. D.; Christensen, J. J.; Sen, D. *Chem. Rev.* **1985**, *85*, 271–339.
- (48) Lamb, J. D.; Smith, R. G. *Talanta* **1992**, *39*, 923–930.
- (49) Smith, R. G.; Drake, P. A.; Lamb, J. D. *J. Chromatogr.* **1991**, *546*, 139–149.
- (50) Lamb, J. D.; Smith, R. G.; Jagodzinski, J. *J. Chromatogr.* **1993**, *640*, 33–40.
- (51) Pirkle, W. H.; Pochapsky, T. C. *Chem. Rev.* **1989**, *89*, 347–362.